Application of hybrid nanofluid and a twisted turbulator in a parabolic solar trough collector: Energy and exergy models

Yacine Khetib [a,b,*], Ali Alzaed [c], Ahmad Alahmadi [d], Goshtasp Cheraghian [e], Mohsen Sharifpur [f,g,*]

[a] Mechanical Engineering Department, Faculty of Engineering, King Abdulaziz University, Jeddah 80204, Saudi Arabia
[b] Center excellence of renewable energy and power, King Abdulaziz University, Jeddah 80204, Saudi Arabia
[c] Architectural Engineering Department, Faculty of Engineering, Taif University, Taif, Saudi Arabia
[d] Department of Electrical Engineering, College of Engineering, Taif University, Taif 21944, Saudi Arabia
[e] Technische Universität Braunschweig, Braunschweig, Germany
[f] Department of Mechanical and Aeronautical Engineering, University of Pretoria, Pretoria, 0002, South Africa
[g] Department of Medical Research, China Medical University Hospital, China Medical University, Taichung, Taiwan

ARTICLE INFO

Keywords:
Twisted turbulator
Two-phase flow
Solar collector
Numerical solution
Exergy and energy Efficiency
k-ε model

ABSTRACT

The impact of a twisted turbulator in a parabolic solar collector on the improvement of thermal–hydraulic performance (THP), as well as energy and exergy Efficiency of MgO-Cu/water hybrid nanofluid (HNF) is numerically evaluated. The main goal of this study is to use a twisted turbulator with pitch ratios (γ) of 1, 1.5, 2, and 2.5 for Reynolds numbers (Re) of 8000 to 32,000 and volume fractions (ϕ) of 1, 2, and 3% of MgO and Cu nanoparticles. Numerical simulation findings are reported in the form of graphs of average Nusselt number (Nu_{ave}), pressure drop (Δp), THP, energy Efficiency (η_c), and exergy Efficiency (η_{ex}). It can be concluded that Nu_{ave} and Δp depends on ϕ and Re and augments linearly with their values. Moreover, Nu_{ave} and Δp increases significantly by increasing the pitch ratio of the turbulator. The results revealed that the maximum values of augmentation of η_c and η_{ex} are respectively 23.79% and 21.15% by raising Re from 8000 to 32000. In a SC with a turbulator with $\gamma = 2$ and $\phi = 3\%$, η_c is raised by 24.16% by increasing Re from 8000 to 32000; while, in the case of $\gamma = 2.5$ and $\phi = 3\%$, η_c is enhanced by 18.2%.

Introduction

The sun is always one of the most energetic resources available to humans without causing pollution. Therefore, its use has attracted the attention of researchers and led them to provide a variety of methods of using it in the best possible way [1–7]. Many researchers in recent years have sought to reduce energy consumption in various devices [8–12]. They have conducted their studies using laboratory or numerical methods [13–17]. One of the most important issues for researchers is solar collectors and research to increase their thermal efficiency [18–21]. One of the main parts of solar collectors is their tubes and also the operating fluid flowing in them that act as heat exchanger [22–24]. One of the proposed alternative fluids is nanofluids. In fact, there have been many reports of how nanofluids function positively [25–28]. Today, many researchers have used nanotechnology in their research [29–34]. The use of nanoparticles is used in many scientific fields today [35–41]. Addition of nanoparticles and creation of nanofluids is also one of the applications of nanotechnology in heat transfer [43,42]. In recent years, many researchers have used nanofluids in their research [47–51]. Many of these researchers have stated that the use of nanofluids can lead to better heat transfer in different heating devices [52,53].

Many researchers have also tried to modify the structure of the pipe to increase the thermal efficiency of the collectors and also to use nanofluids as the working fluid [54–59]. In this way, Skullong et al. [60] numerically investigated the effect of the vortex generators inside the solar heater using the finite volume method (FVM). In this study, they used SOLIDWORKS software to model the geometry of the solar heater. They also employed FLUENT software to analyze the fluid flow. Their results demonstrated that the use of vortex generators causes the form of the streamlines near the walls to change, which leads to the formation of

* Corresponding authors at: Mechanical Engineering Department, Faculty of Engineering, King Abdulaziz University, Jeddah 80204, Saudi Arabia (Y. Khetib). Department of Mechanical and Aeronautical Engineering, University of Pretoria, Pretoria, 0002, South Africa (M. Sharifpur).
E-mail addresses: ykhetib@yahoo.com, ykhateb@kau.edu.sa (Y. Khetib), mohsen.sharifpur@up.ac.za (M. Sharifpur).

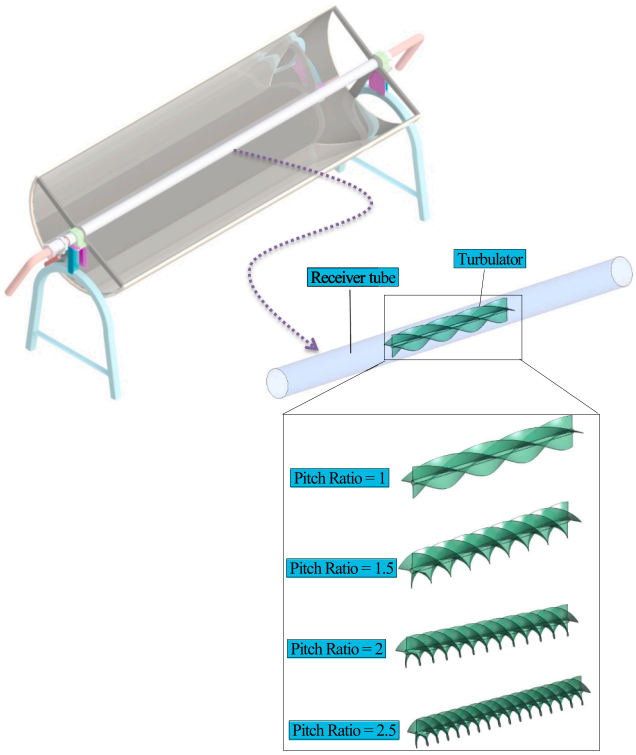

Fig. 1. Schematic of SC with twisted turbulator.

Table 1
Physical properties of base fluid and nanoparticles [74,75].

Property	MgO	Cu	water
$\rho(kg.m^{-3})$	3560	8954	998.2
$c_P(J.kg^{-1}.K^{-1})$	955	383	4182
$k(W.m^{-1}.K^{-1})$	45	400	0.6
$\mu(kg.m^{-1}.s^{-1})$	–	–	0.001003

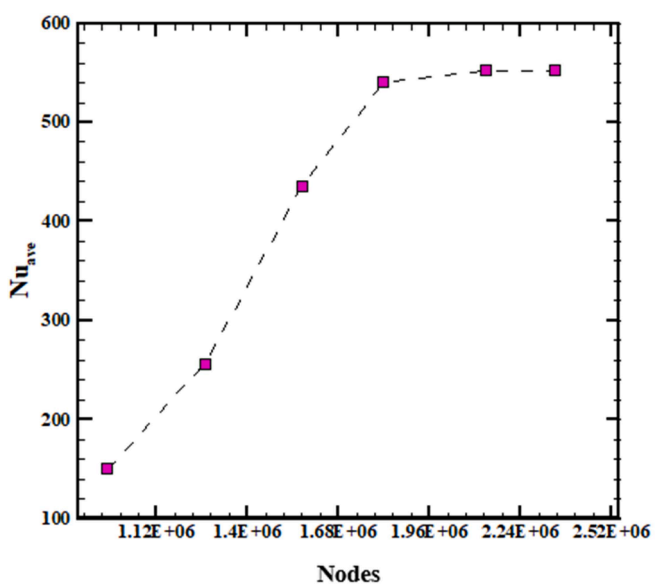

Fig. 2. Nu_{ave} for Re = 32000, ϕ = 3%, γ = 2.5, and different grid resolutions.

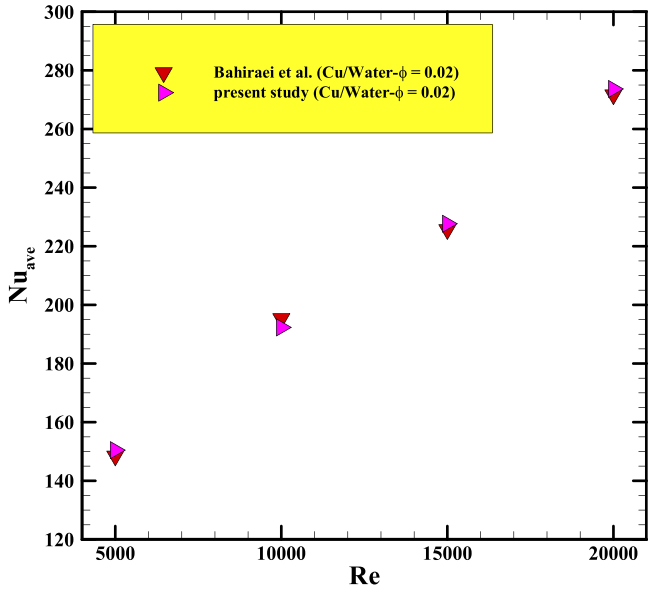

Fig. 3. Validation and comparison of the present numerical simulation by results of Bahirai et al. [79].

vortices and increment of heat transfer.

Sheikholeslami and Farshad [61] numerically investigated the effect of novel turbulators on the THP of a HNF flowing in a SC. They used FLUENT software to model and analyze the performance of the SC in turbulent flow regime for Re ranging from 6,000 to 24,000 using the k-ε turbulence model. It was shown that the use of turbulators leads to the higher mixing and creation of turbulence in the HNF flow, which improves the thermal performance of the SC.

Sheikholeslami et al. [62] numerically investigated the effect of hybrid turbulators on the nanofluid entropy generation in a SC using the FVM and ANSYS FLUENT software. They revealed that the entropy generation diminishes with the step and pitch ratio.

Saedodin et al. [63] numerically explored the effect of twisted tapes on the thermal performance of parabolic SCs using the FVM. In this study, the effect of pitch ratio and longitudinal ratio of twisted tapes on the THP of SC was investigated. The authors reported that the maximum heat transfer rate in the SC with twisted tape is 51.43%. Also, an enhancement of the twisted tapes and their longitudinal ratio improves the thermal performance of the collector.

Olfian et al. [64] analyzed the effect of twisted tapes on the thermal performance of SCs containing phase change materials using computational fluid dynamics and FLUENT software. They used the SIMPLEC algorithm and showed that the maximum thermal Efficiency of the SC with twisted tapes and phase change materials is 22.78%.

Farshad and Sheikholeslami [65] evaluated the effect of hybrid turbulators on η_{ex} of water-aluminum oxide nanofluid in a linear parabolic SC using FVM and computational fluid dynamics. They used FLUENT software for modeling. It was concluded that the use of a rotary turbulator significantly improves η_{ex} compared to the parabolic SC without a hybrid turbulator. Also, the use of water-aluminum oxide nanofluid is more suitable than the base fluid in terms of η_{ex}. In addition, the maximum η_{ex} of the collector with a hybrid turbulator was 34.61%.

Ghasemi and Ranjbar [66] evaluated the effect of porous plates on the THP of parabolic SCs using FVM and FLUENT software. The effect of diameter, size, and spacing of porous holes on the THP of a parabolic SC was discussed. it was revealed that changing the distance and size of porous holes improves the thermal performance of the parabolic SC. Also, the thermal Efficiency of the parabolic SC was enhanced up to 48.11% when porous plates were employed.

Oztop et al. [67] theoretically studied the effect of geometry,

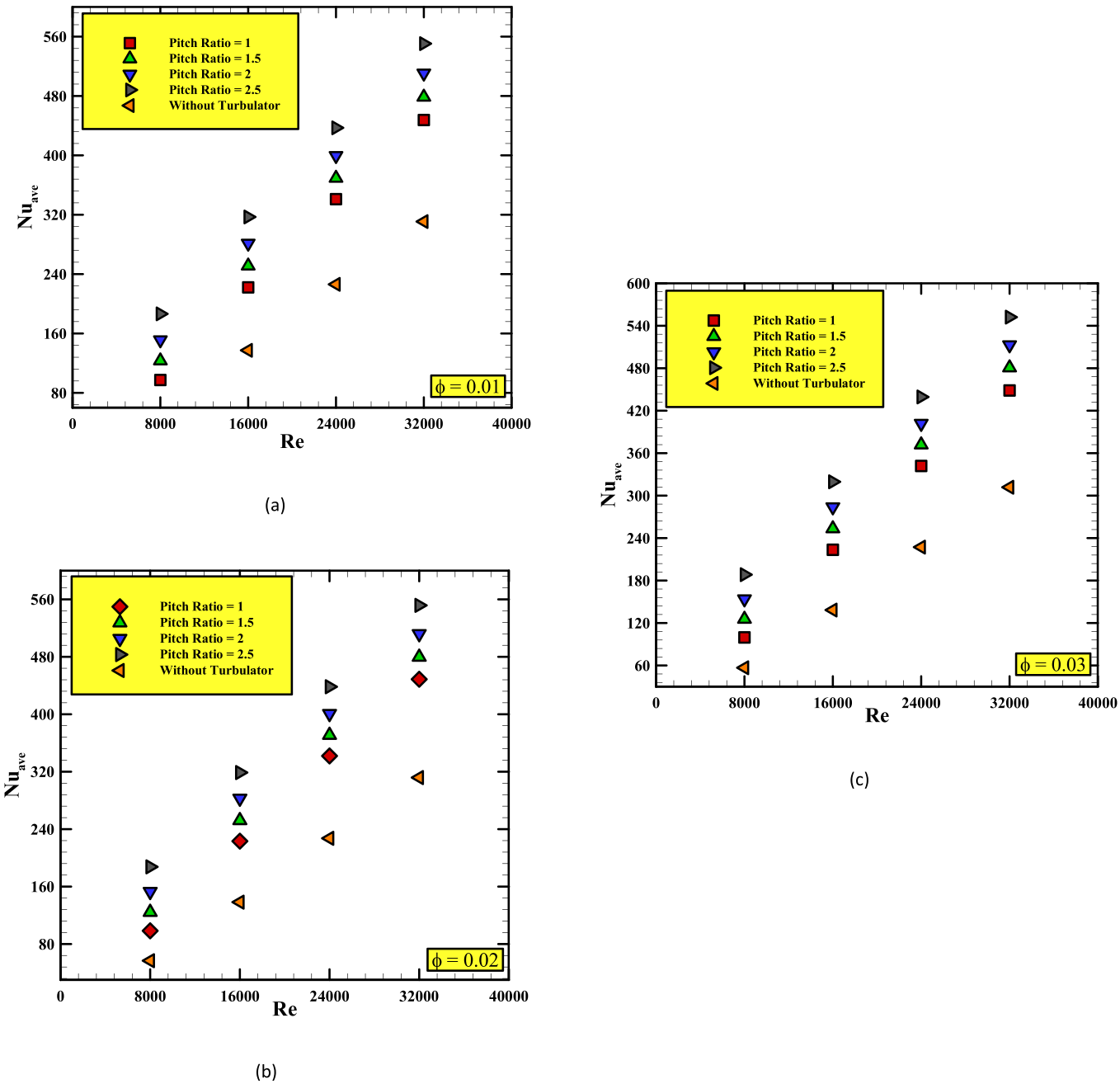

Fig. 4. Nu_{ave} versus Re in a parabolic SC equipped with a twisted turbulator with different pitch ratios for (a) $\phi = 1\%$, (b) $\phi = 2\%$, and (c) $\phi = 3\%$.

material, type of fluid and nanofluid on η_{ex} and η_c in SCs. It was demonstrated that η_{ex} and η_c are strongly influenced by geometric parameters. They reported that the maximum improvement in η_c and η_{ex} is between 17% and 91%.

Balaji et al. [68] experimentally considered the absorber tubes to improve the thermal performance of the SC and found that they have a significant effect on improving the thermal performance of the SC.

Acir et al. [69] numerically studied the impact of various turbulator angles on η_c and η_{ex} of a parabolic SC using computational fluid dynamics and FLUENT software. Their study was carried out in turbulent flow regime and Re ranging from 5000 to 25000. They used the k-ω turbulence model and showed that increment of the turbulator angle and Re enhances η_{ex} and η_c of the parabolic SC.

Rostami et al. [70] numerically studied the effect of using a tube with an elliptical cross section inside a SC filled with nanofluid to evaluate the effect of an elliptical cross-section tube on η_{ex} of a SC for Re = 5000 to 20,000 and $\phi = 1$ to 4%. Their results indicated that η_{ex} of the SC with elliptical cross section tubes is higher than that with circular one. Also, the maximum η_{ex} of SC was reported to be 17.11%.

Goldanlou et al. [71] evaluated the effect of using HNF on hydraulic parameters of a parabolic SC using FLUENT software and FVM. In order to model the flow and discretization of the equations, they used k-ω turbulence model and SIMPLEC algorithm, respectively. It was revealed that Nu_{ave} is an ascending function of Re and ϕ. Also, the maximum increase in thermal performance in this study was 46.89%.

Nazir et al. [72]analyzed the effect of alumina nanofluid on η_{ex} in a parabolic SC numerically using the FVM and FLUENT software. They employed structured mesh and ANSYS meshing software to grid the geometry of the SC. Their results revealed that η_{ex} of the parabolic SC is influenced by Re and ϕ.

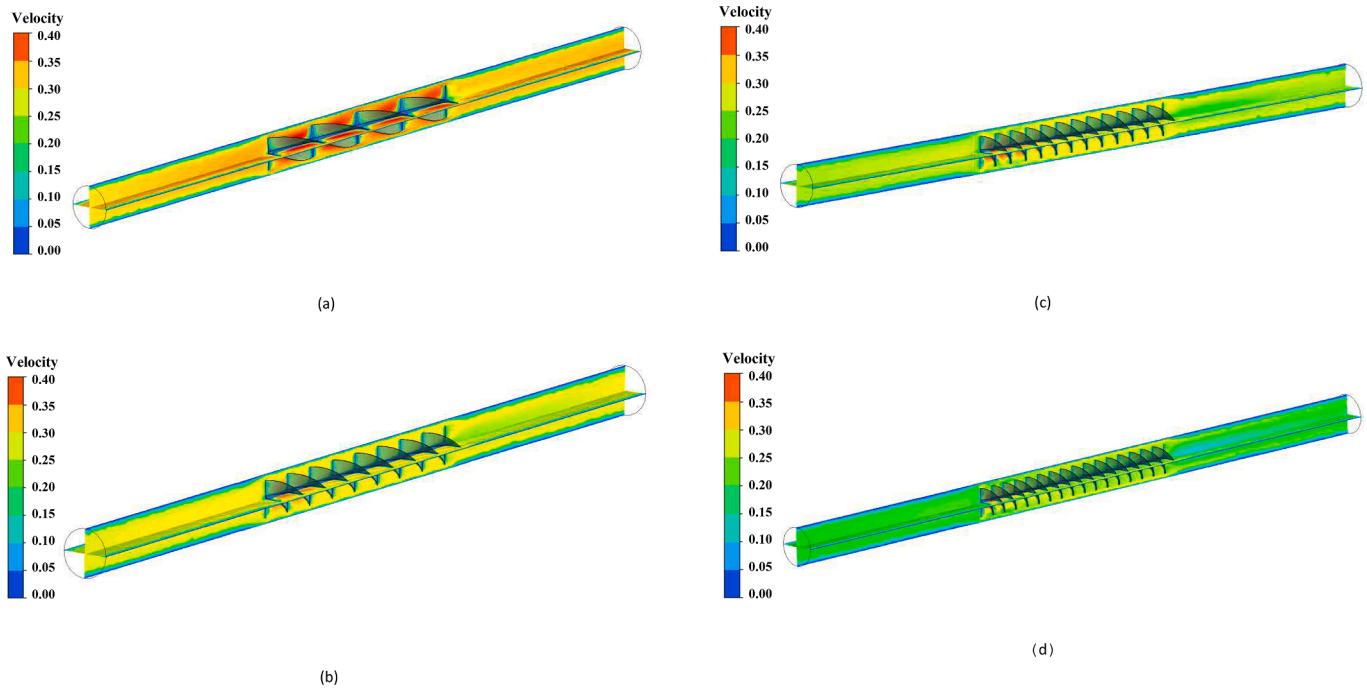

Fig. 5. Velocity contours of TPHNF flow within a parabolic SC equipped with a twisted turbulator for a fraction of 3%, Re = 32000, and (a) $\gamma = 1$, (b) $\gamma = 1.5$, (c) $\gamma = 2$, and (d)) $\gamma = 2.5$.

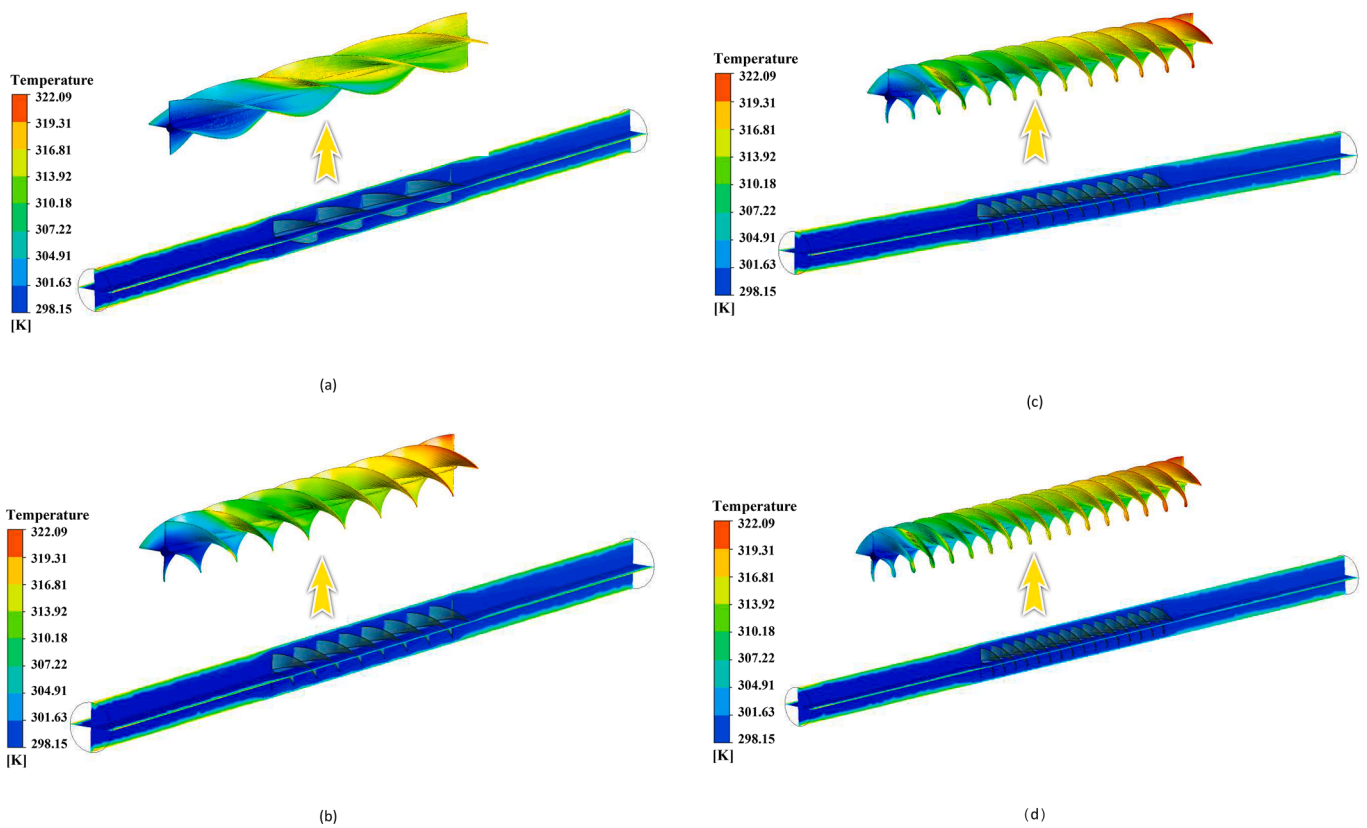

Fig. 6. Temperature contours of TPHNF flow within a parabolic SC equipped with a twisted turbulator for a fraction of 3%, Re = 32000, and (a) $\gamma = 1$, (b) $\gamma = 1.5$, (c) $\gamma = 2$, and (d)) $\gamma = 2.5$.

Ma et al. [73] used the FVM to analyze the effect of hot and cold heat sources on the THP of an adiabatic tube using FLUENT software. They used structured mesh and ANSYS meshing software to grid the geometry. Their results showed that Nu_{ave} is enhanced linearly with the Rayleigh number and ϕ.

Dezfulizadeh et al. [74] used FLUENT software to model the geometry of dual-pipe heat exchangers equipped with grooved helical turbulators. They investigated the effect of different geometric shapes of

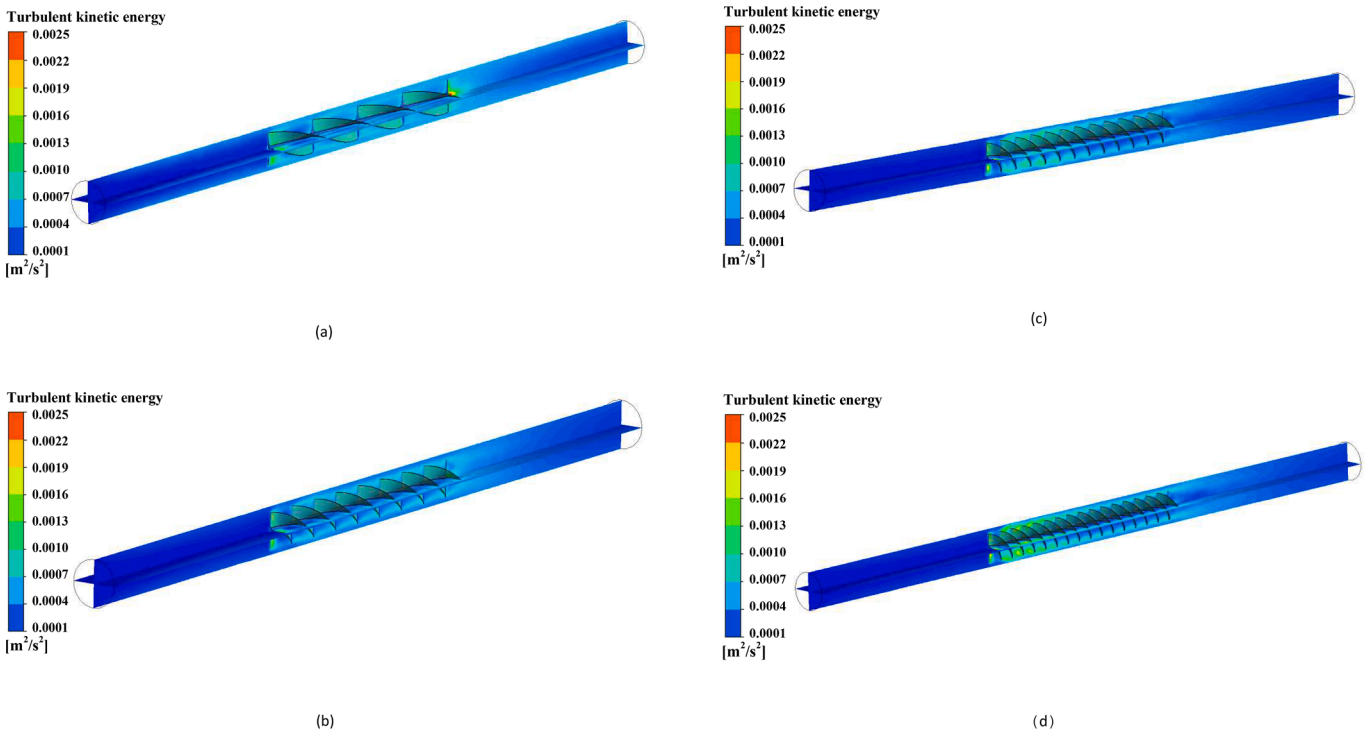

Fig. 7. Turbulent kinetic energy contours of TPHNF flow within a parabolic SC equipped with a twisted turbulator for a fraction of 3%, Re = 32000, and (a) $\gamma = 1$, (b) $\gamma = 1.5$, (c) $\gamma = 2$, and (d)) $\gamma = 2.5$.

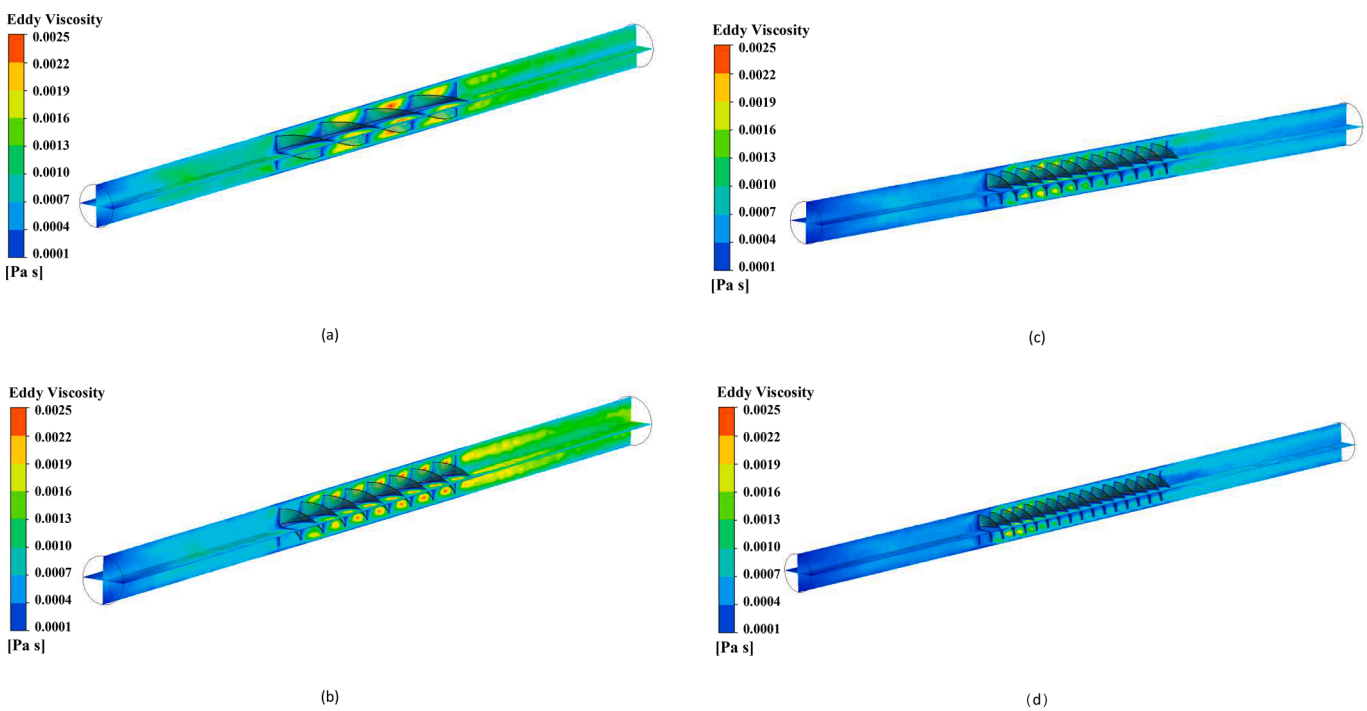

Fig. 8. Turbulent viscosity contours of TPHNF flow within a parabolic SC equipped with a twisted turbulator for a fraction of 3%, Re = 32000, and (a) $\gamma = 1$, (b) $\gamma = 1.5$, (c) $\gamma = 2$, and (d)) $\gamma = 2.5$.

grooves and reported that spherical shape of grooves is desirable in terms of η_{ex}. Also, the maximum η_{ex} in this study was reported to be 45.11%.

According to the studies conducted so far, the effect of using a twisted turbulator on THP, η_{ex} and η_c of two-phase MgO-Cu/water HNF in a parabolic SC has not been studied. The innovations of this study are the use of hybrid nanofluids in parabolic SCs, the study of a new geometry of turbulators with different parameters, the introduction of turbulent viscosity and turbulent kinetic energy contours for the analysis of the mentioned results. Therefore, in this numerical study, the effect of two-phase MgO-Cu/water HNF with $\phi = 1$ to 3%, Re = 8000 to 32000, and pitch ratios of 1, 1.5, 2, and 2.5 is evaluated in turbulent flow

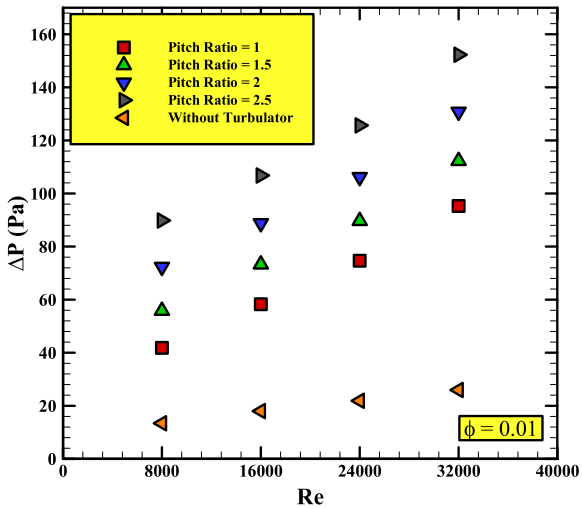

(a)

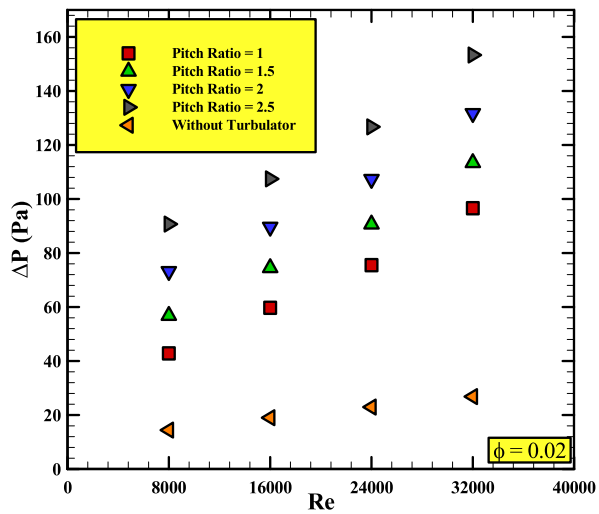

(b)

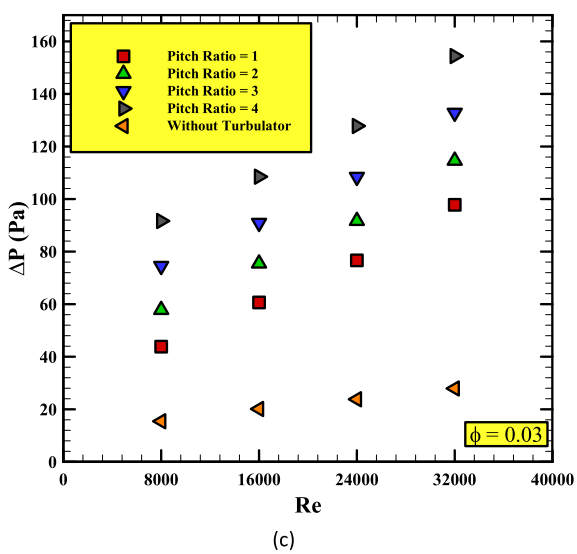

(c)

Fig. 9. Δp versus Re for a parabolic SC equipped with a twisted turbulator with different pitch ratios and (a) ϕ = 1%, (b) ϕ = 2%, and (c) ϕ = 3%.

regime.

Geometric model and governing equations

The geometry of the parabolic SC with twisted turbulator is shown schematically in Fig. 1. The length of the absorber tube is 1000 mm, and the length of the twisted turbulator is 300 mm. Also, the distance between the turbulator and collector inlet and outlet is 350 mm.

The two-phase MgO-Cu/water HNF is used as the working fluid. The thermophysical properties of the base fluid (water) and nanoparticles are presented in Table 1.

In order to simulate the MgO-Cu/water nanofluid flow inside the SC, the two-phase mixed model is employed.

In this study, the flow is considered turbulent, incompressible, steady and three-dimensional.

Equations and relations are followed as [76–78]:

The continuity equation:

$$\nabla\left(\rho_m \vec{U}_m\right) = 0\vec{U}_m = \frac{\rho_s\phi_s\vec{U}_s + \rho_{bf}\phi_{bf}\vec{U}_{bf}}{\rho_m}\rho_m = \rho_s\phi_s + \rho_{bf}\phi_{bf} \tag{1}$$

The steady-state momentum equation:

$$\rho_m\left(\vec{U}_m\nabla\vec{U}_m\right) = -\nabla\vec{P} + \mu_m\left(\nabla\vec{U}_m + \left(\nabla\vec{U}_m\right)^T\right) + \nabla\left(\rho_{bf}\phi_{bf}\vec{U}_{dr,bf}\vec{U}_{dr,bf} + \rho_s\phi_s\vec{U}_{dr,s}\vec{U}_{dr,s}\right) + \rho_m\vec{g} \tag{2}$$

$$\vec{U}_{dr,bf} = \vec{U}_{bf} - \vec{U}_m\vec{U}_{dr,s} = \vec{U}_s - \vec{U}_m \tag{3}$$

The steady-state energy equation:

$$\nabla\left(\rho_{bf}\phi_{bf}\vec{U}_{bf}h_{bf} + \rho_s\phi_s\vec{U}_s h_s\right) = \nabla\left(\left(\phi_{bf}k_{bf} + \phi_s k_s\right)\nabla\vec{T}\right) \tag{4}$$

The volume fraction equation for two-phase mixture:

$$\nabla\left(\rho_s\phi_s\vec{U}_m\right) = -\nabla\left(\rho_s\phi_s\vec{U}_{dr,s}\right) \tag{5}$$

$$\vec{U}_{bf,s} = \vec{U}_{bf} - \vec{U}_s \tag{6}$$

$$\vec{U}_{dr,s} = \vec{U}_{s,bf} - \frac{\rho_s\phi_s}{\rho_m}\vec{U}_{bf,s} \tag{7}$$

$$\vec{U}_{bf,s} = \frac{d_p^2}{18\mu_{bf}\not{f}_d}\frac{\rho_s - \rho_m}{\rho_s}\vec{\alpha} \tag{8}$$

$$\not{f}_d = 1 + 0.15\mathrm{Re}_s^{0.687} \tag{9}$$

$$\vec{\alpha} = \vec{g} - \left(\vec{U}_m\nabla\vec{U}_m\right) \tag{10}$$

$$\mathrm{Re}_s = \frac{\vec{U}_m d_p\rho_m}{\mu_m} \tag{11}$$

$$\eta_c = \frac{E_c}{I\bullet A} = \frac{Q_{in}\bullet\rho_{in}\bullet c_{p,in}\bullet(T_{out} - T_{in})}{6\bullet 10^4\bullet I\bullet A} \tag{12}$$

$$\eta_{ex} = \frac{\dot{Q}_{HTF} - \dot{m}_{HTF}c_{p,HTF}\ln\left(\frac{T_\infty}{T_{i,HTF}}\right)}{-\dot{Q}_{HTF} - \dot{m}_{CF}c_{p,CF}\ln\left(\frac{T_{o,CF}}{T_{i,CF}}\right) + VI\eta_P} \tag{13}$$

Numerical simulation

In this study, the FVM is used to perform the simulations. Three-dimensional geometry of the SC is generated using the design modeler

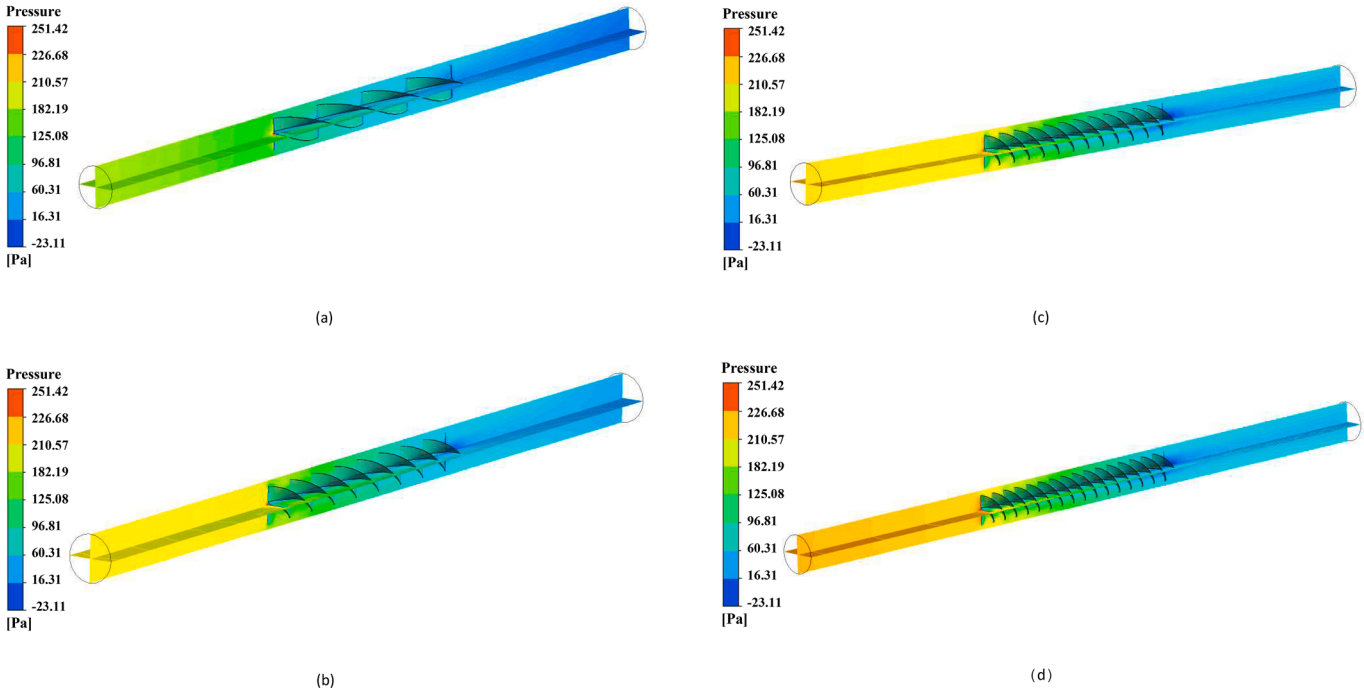

Fig. 10. Pressure contours of TPHNF for $\phi = 3\%$, Re = 32000, and (a) $\gamma = 1$, (b) $\gamma = 1.5$, (c) $\gamma = 2$, and (d) $\Gamma = 2.5$.

software. Then, the geometry is created using ANSYS Mashing software. After doing the grid study, the grid is exported into FLUENT software. The MgO-Cu/water HNF is modeled by employing the two-phase Eulerian-Eulerian model. The first and second phases are water and MgO-Cu nanoparticles. Since 8000 < Re < 32000, the turbulent flow regime is modeled using the standard k-ε approach. The SIMPLE algorithm is used for coupling the velocity and pressure fields. The Least Squares Cell Based model is employed to spatially discretize the gradients. The PRESTO model is also used to discretize the pressure, and the first-order upwind scheme is employed for momentum, volume fraction, and turbulent kinetic energy equations.

Grid study

An appropriate grid should be selected to ensure the results are independent of the grid elements. Hence, Nu_{ave} is calculated for MgO-Cu/water two-phase hybrid nanofluid (TPHNF) for different number of grid points (Fig. 2). This figure shows that a grid with 2,132,168 nodes is sufficient for the present simulations. Because as the number of grid points is enhanced, Nu_{ave} does not change significantly.

Validation

The present numerical results are verified by using the results of Bahirai et al. [79]. Nu_{ave} is calculated and compared with their reported data (Fig. 3). The figure demonstrates that the difference between values of Nu_{ave} obtained from the present simulations and those reported by Bahirai et al. [79] is about 2.09%, confirming that the curacy of the results is ensured.

Results and discussion

The numerical results of the present simulations are provided in this section. The impact of different pitch ratios of the turbulator on Nu_{ave}, Δp, THP, and η_c and η_{ex} is investigated. Also, the contours of velocity, temperature, pressure, and streamlines are presented for pitch ratios of 1, 1.5, 2, and 2.5, $\phi = 3\%$, and Re = 32000.

Effect of pitch ratio on Nu_{ave}

Fig. 4 illustrates Nu_{ave} versus Re in a SC equipped with a twisted turbulator with different pitch ratios and different values of $\phi = 1\%$, 2%, and 3%. Nu_{ave} depends on the volume fraction of nanoparticles and Re and is enhanced linearly with their magnitudes. Besides, Nu_{ave} intensifies with the pitch ratio significantly.

As the pitch ratio increases, the turbulence in the nanofluid flow increases, resulting in increased heat transfer. For $\phi = 1\%$ and Re = 32000, the placement of twisted turbulators with $\gamma = 2.5$ within the parabolic SC leads to an increment in Nu_{ave} by 92.01% compared to the parabolic SC without turbulator. For $\phi = 2\%$ and Re = 32,000, the placement of twisted turbulators with $\gamma = 2.5$ within the parabolic SC raises Nu_{ave} by 93.27% compared to the parabolic SC without turbulator. When $\phi = 3\%$ and Re = 32,000, the placement of twisted turbulators with $\gamma = 2.5$ within the parabolic SC leads to an enhancement in Nu_{ave} by 94.70% compared to the parabolic SC without turbulator.

Velocity contours of TPHNF flow within a parabolic SC are presented in Fig. 5 for $\phi = 3\%$, Re = 32000, and different pitch ratios of 1, 1.5, 2, and 2.5. It can be concluded that due to no-slip boundary condition, the velocity of two-phase MgO-Cu/water HNF is zero close to the wall. In the middle of the SC, however, the velocity of two-phase MgO-Cu/water HNF is enhanced due to mixing and turbulence generated by the twisted turbulator.

Fig. 6 reveals the temperature contours for the TPHNF for a fraction of 3%, Re = 32000, and different pitch ratios of 1, 1.5, 2, and 2.5. The temperature of the HNF intensifies the surface temperature of the twisted turbulator by passing through the parabolic SC and receiving the solar radiation energy.

Turbulent kinetic energy contours are plotted in Fig. 7 for a fraction of 3%, Re = 32000, and different pitch ratios of 1, 1.5, 2, and 2.5. The amount of turbulent kinetic energy in the areas between the turbulator blades is enhanced with the pitch ratio.

The amount of turbulent kinetic energy indicates the kinetic energy of the turbulence and is due to the oscillating terms of the velocity in the turbulent flow. As the amount of turbulence in the flow increases with increasing γ, the amount of turbulent kinetic energy caused by the turbulence also increases.

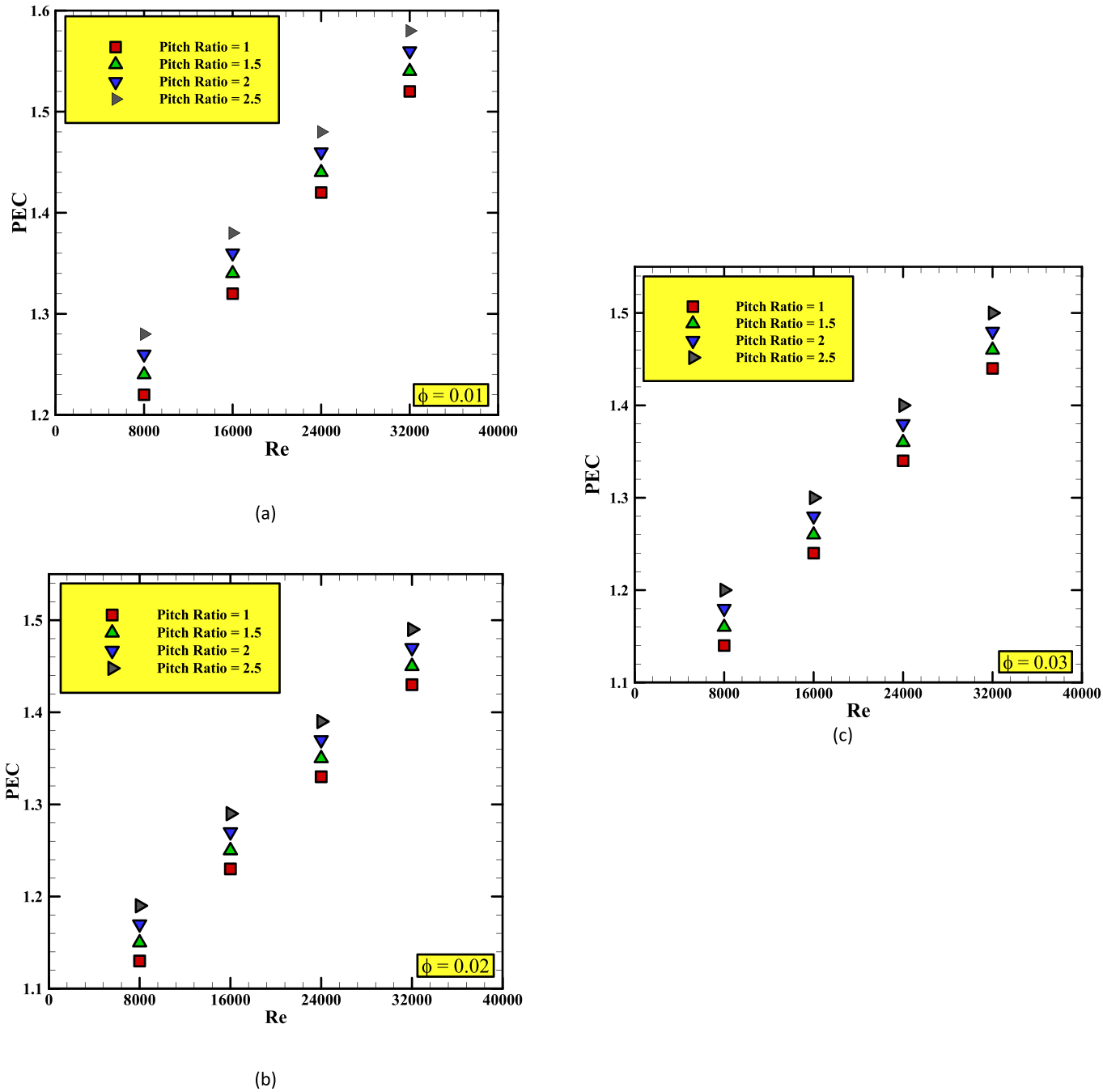

Fig. 11. The variations of THP as a function of Re is shown in Fig. 11 for a parabolic SC equipped with a twisted turbulator for different pitch ratios and (a) $\phi = 1\%$, (b) $\phi = 2\%$, and (c) $\phi = 3\%$.

Fig. 8 demonstrates the turbulent viscosity contours for TPHNFs for a fraction of 3%, Re = 32000, and different pitch ratios of 1, 1.5, 2, and 2.5. As can be observed, the maximum amount of turbulent viscosity occurs between the blades of the twisted turbulator due to the rotational motion of the vortices. The increase in turbulent viscosity is also due to the increase in turbulence caused by flow fluctuations. The formation of flow fluctuations is also due to the presence of turbulators.

Effect of pitch ratio on Δp

Fig. 9 reveals Δp versus Re in a parabolic SC equipped with a twisted turbulator with different pitch ratios and $\phi = 1\%$, 2%, and 3%. It is found that Δp depends on ϕ and Re and is enhanced linearly with their values with a relatively sharp slope. Besides, the amount of Δp is intensified significantly by raising the pitch ratio. For $\phi = 1\%$ and Re = 32000, twisted turbulators with $\gamma = 2.5$ improves Δp by 387.11% compared to the parabolic SC without turbulator. When $\phi = 2\%$ and Re = 32000, twisted turbulators with $\gamma = 2.5$ intensifies Δp by 388.45% compared to the parabolic SC without turbulator. For $\phi = 3\%$ and Re = 32000, twisted turbulators with $\gamma = 2.5$ leads to an enhancement in Δp by 389.62% compared to the parabolic SC without turbulator.

Pressure contours of TPHNFs are presented in Fig. 10 for $\phi = 3\%$, Re = 32000, and different pitch ratios of 1, 1.5, 2, and 2.5. It is found that an enhancement in the pitch ratio of the twisted turbulator intensifies the accumulation of TPHNF flow when collides with the turbulator, resulting in an increment in the density of streamlines and an

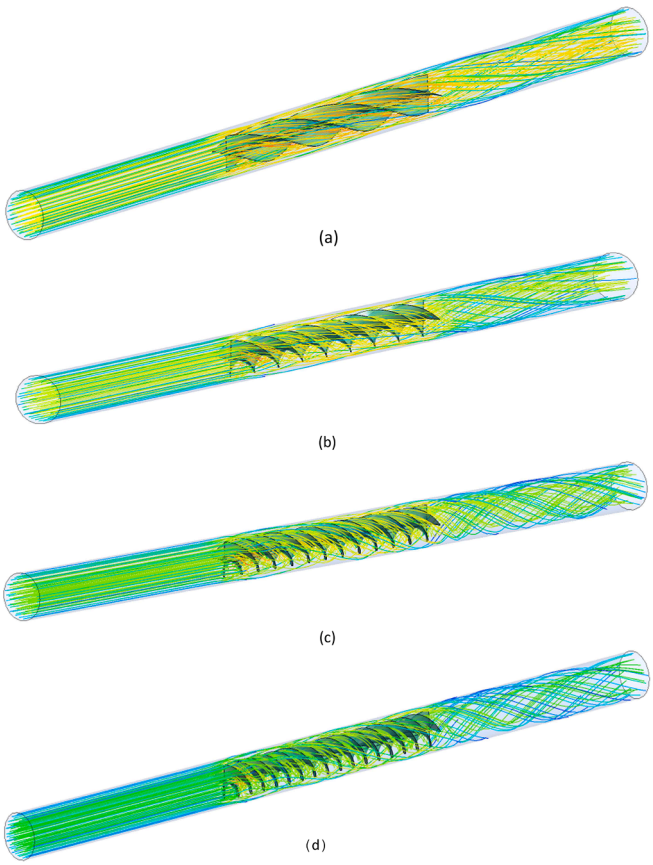

Fig. 12. Streamline contours for TPHNF flow when the fraction is 3% and Re = 32000 for (a) $\gamma = 1$, (b) $\gamma = 1.5$, (c) $\gamma = 2$, and (d) $\gamma = 2.5$.

enhancement in Δp.

As the pitch ratio increases, the contact surface with the fluid flow increases, resulting in increased shear stresses and pressure drops. On the other hand, due to the presence of the turbulator and the increase of the pitch ratio, the flow lines become more curved and as a result, the pressure drop due to its presence increases.

Effect of pitch ratio on THP

The variations of THP as a function of Re is shown in Fig. 11 for a parabolic SC equipped with a twisted turbulator for different pitch ratios and $\phi = 1\%$, 2%, and 3%. It is observed that the values of the THP are greater than 1 for all cases, indicating that the addition of a twisted turbulator and raising its pitch ratio are desirable for improving the THP. As the Reynolds number increases, the amount of heat transfer increases, and as a result, the amount of PEC also increases.

The contours of streamlines are plotted in Fig. 12 for TPHNF flow when the fraction is 3% and Re = 32000 for various pitch ratios of 1, 1.5, 2, and 2.5. The figure demonstrates that the density of the streamlines is intensified with the pitch ratio in a twisted turbulator.

Effect of pitch ratio on η_c

Fig. 13 shows η_c as a function of Re in a parabolic SC equipped with a twisted turbulator for different values of ϕ and pitch ratios of 1, 1.5, 2, and 2.5. For all cases, η_c is affected by Re and ϕ and is enhanced linearly with them significantly. In a SC with a turbulator with $\gamma = 1$ and $\phi = 3\%$, the amount of η_c increases by 23.11% by raising Re from 8000 to 32000. In a SC with a turbulator with $\gamma = 1.5$ and $\phi = 3\%$, the amount of η_c is intensified by 23.79% by enhancing Re from 8000 to 32000. In a SC with a turbulator with $\gamma = 2$ and $\phi = 3\%$, the amount of η_c is raised by 24.16% by increasing Re from 8000 to 32000. In a SC with a turbulator with $\gamma = 2.5$ and $\phi = 3\%$, the amount of η_c is enhanced by 18.2% by raising Re from 8000 to 32000.

Effect of pitch ratio on η_{ex}

η_{ex} as a function of Re is illustrated in Fig. 14 for a parabolic SC equipped with a rotary turbulator with different values of ϕ and pitch ratios of 1, 1.5, 2, and 2.5. The figure demonstrates that η_{ex} is affected by the volume fraction and Re and is enhanced with them. However, η_{ex} is reduced with the pitch ratio. In a SC with a turbulator with $\gamma = 1$ and $\phi = 3\%$, the amount of η_{ex} is raised by 21.15% by enhancing Re from 8000 to 32000. In a SC with a turbulator with $\gamma = 1.5$ and $\phi = 3\%$, the amount of η_{ex} is enhanced by 20.83% by raising Re from 8000 to 32000. In a SC with a turbulator with $\gamma = 2$ and $\phi = 3\%$, the amount of η_{ex} is improved by 19.26% by enhancing Re from 8000 to 32000. In a SC with a turbulator with $\gamma = 2.5$ and $\phi = 3\%$, the amount of η_{ex} is enhanced by 18.70% by improcing Re from 8000 to 32000.

Conclusions

In this study, the impact of using a twisted turbulator on THP of a collector, η_c and η_{ex} of MgO-Cu/water HNF was evaluated by considering a two-phase model for HNF in a parabolic SC. Based on the results obtained from the numerical study, the following conclusions can be expressed:

- The amount of Δp is enhanced significantly by raising the pitch ratio.
- For all cases, the values of the THP are greater than 1, showing that the addition of twisted turbulator and enhancing its pitch ratio can improve the THP.
- For all cases, η_c is affected by Re and ϕ and is enhanced significantly as they are raised.
- In a SC with a turbulator with $\gamma = 2.5$ and $\phi = 3\%$, the amount of η_c is enhanced by 18.2% by intensifying Re from 8000 to 32000.
- η_{ex} is affected by ϕ and Re and is raised as they are enhanced. However, η_{ex} is reduced by enhancing the Reynolds number from 8000 to 32000.
- In a SC with a turbulator with $\gamma = 1$ and $\phi = 3\%$, the amount of η_{ex} is raised by 21.15% by enhancing Re from 8000 to 32000.

To continue this study and conduct future studies, the following suggestions are provided:

1. Review of new geometries for used turbulators
2. Using other turbulence models and comparing their results with experimental results
3. Comparison of the effect of using different nanofluids on changes in energy and exergy efficiencies

CRediT authorship contribution statement

Yacine Khetib: Methodology, Writing – original draft. **Ali Alzaed:** Software, Validation. **Ahmad Alahmadi:** Writing - review & editing. **Goshtasp Cheraghian:** Writing - review & editing. **Mohsen Sharifpur:** Writing - review & editing, Conceptualization.

Declaration of Competing Interest

The authors declare that they have no known competing financial interests or personal relationships that could have appeared to influence the work reported in this paper.

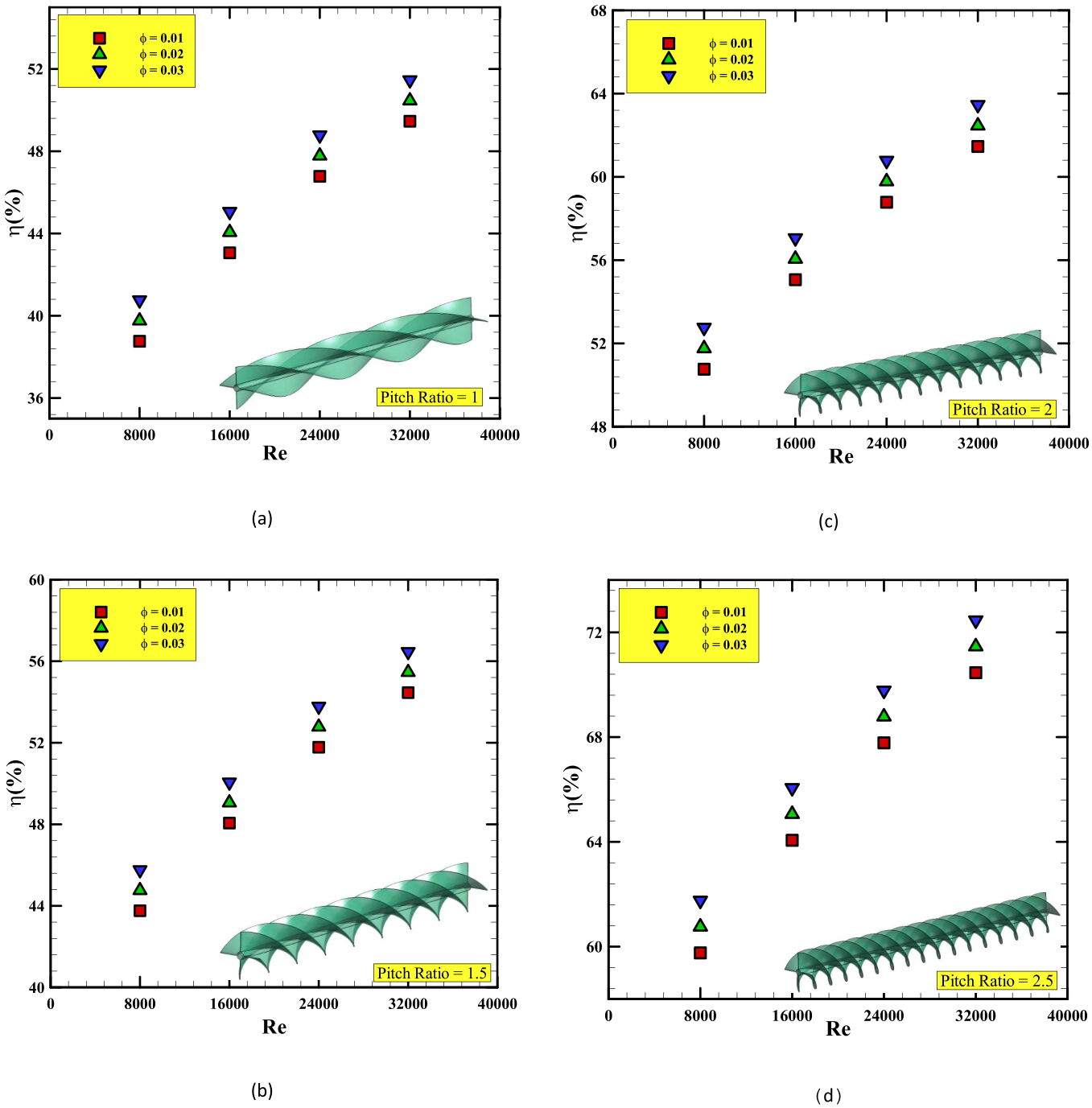

Fig. 13. η_c versus Re in a parabolic SC equipped with a twisted turbulator for different values of ϕ, and (a) γ = 1, (b) γ = 1.5, (c) γ = 2, and (d) γ = 2.5.

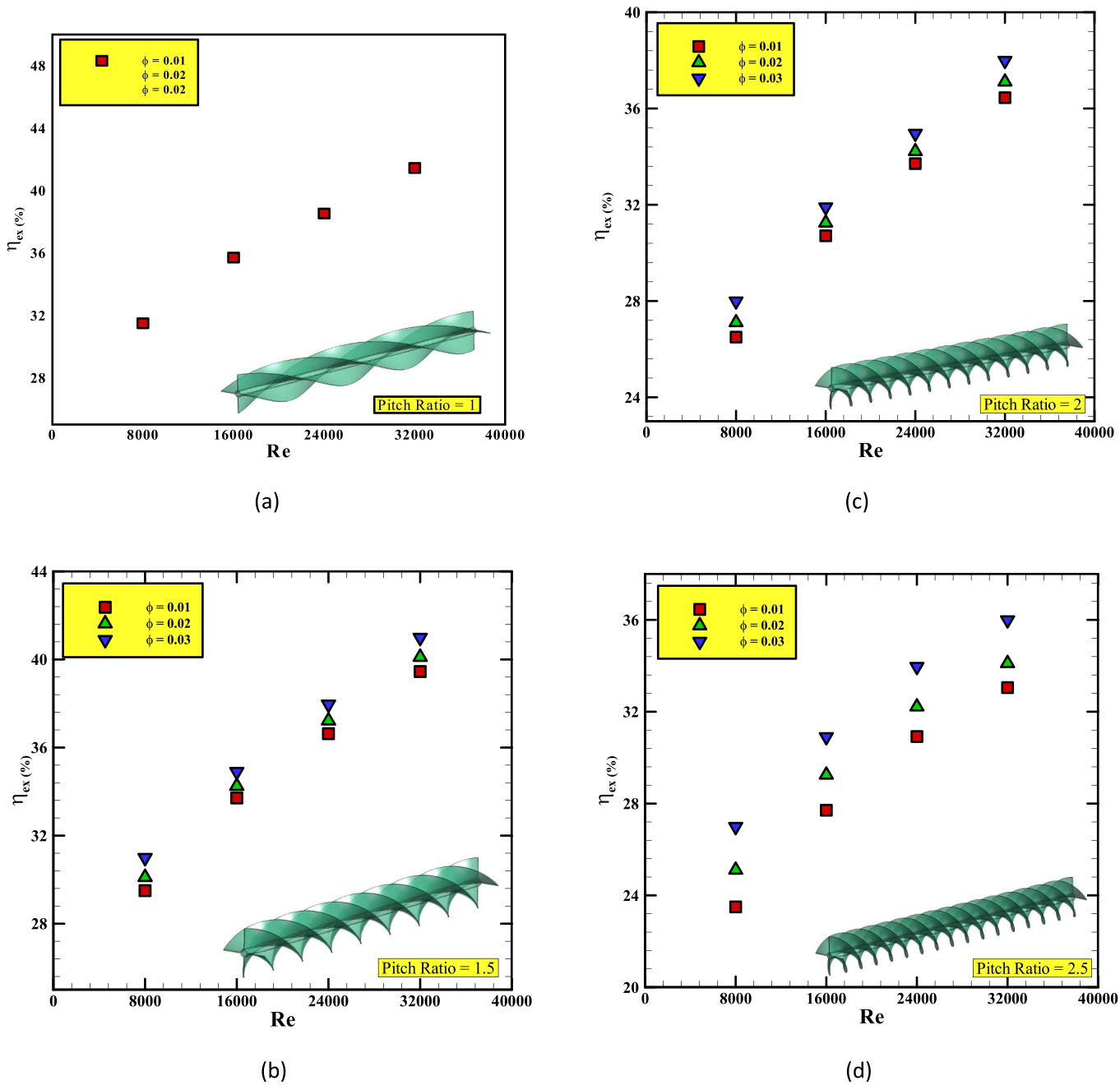

Fig. 14. η_{ex} versus Re for a parabolic SC equipped with a rotary turbulator with different values of ϕ and (a) γ = 1, (b) γ = 1.5, (c) γ = 2, and (d) γ = 2.5.

Acknowledgment

This work was supported by the Taif University Researchers Supporting grant number (TURSP-2020/240) of Taif University, Taif, Saudi Arabia.

References

[1] Attia MEH, et al. Sustainable potable water production from conventional solar still during the winter season at Algerian dry areas: energy and exergy analysis. J Therm Anal Calorim 2020..
[2] Menni Y, Ghazvini M, Ameur H, Ahmadi MH, Sharifpur M, Sadeghzadeh M. Numerical calculations of the thermal-aerodynamic characteristics in a solar duct with multiple V-baffles. Eng Appl Comput Fluid Mech 2020;14(1):1173–97.
[3] Menni Y, Ghazvini M, Ameur H, Kim M, Ahmadi MH, Sharifpur M. Combination of baffling technique and high-thermal conductivity fluids to enhance the overall performances of solar channels. Eng Comput 2020.
[4] Parsa SM. Reliability of thermal desalination (solar stills) for water/wastewater treatment in light of COVID-19 (novel coronavirus "SARS-CoV-2") pandemic: What should consider? Desalination 2021;512:115106.
[5] Parsa SM, et al. First approach on nanofluid-based solar still in high altitude for water desalination and solar water disinfection (SODIS). Desalination 2020;491:114592.
[6] Parsa SM, Rahbar A, Koleini MH, Aberoumand S, Afrand M, Amidpour M. A renewable energy-driven thermoelectric-utilized solar still with external condenser loaded by silver/nanofluid for simultaneously water disinfection and desalination. Desalination 2020;480:114354.
[7] Parsa SM, et al. Effect of Ag, Au, TiO2 metallic/metal oxide nanoparticles in double-slope solar stills via thermodynamic and environmental analysis. J Cleaner Prod 2021;311:127689.
[8] Listiana N, Jaharadak AA. Blended learning as instructional media: Literature review. no. 1, p. 012066. Journal of Physics: Conference Series. IOP Publishing; 2019.
[9] Mosbah A, Ali MA, Aljubari IH, Sherief SR. Migrants in the High-Tech and engineering sectors: An emerging research area. In: 2018 IEEE Conference on Systems, Process and Control (ICSPC). IEEE; 2018. p. 234–7.
[10] Zhang X, Tang Y, Zhang F, Lee CS. A novel aluminum–graphite dual-ion battery. Adv Energy Mater 2016;6(11):1502588.
[11] Wang M, Jiang C, Zhang S, Song X, Tang Y, Cheng H-M. Reversible calcium alloying enables a practical room-temperature rechargeable calcium-ion battery with a high discharge voltage. Nat Chem 2018;10(6):667–72.
[12] Pordanjani AH, et al. Nanofluids: physical phenomena, applications in thermal systems and the environment effects- a critical review. J Cleaner Prod 2021:128573.
[13] Halim S, Mohamad N, Toriman ME, Bakar NHA, Hashim SN, Adnan LHM, et al. Role of Zamzam water as a vital mineral supplement in the treatment of opioid dependence and tolerance. A review. Res J Pharm Technol 2016;9(7):957. https://doi.org/10.5958/0974-360X.2016.00183.9.
[14] Khan J, et al. Development and evaluation of topical emulgel of aspirin using different polymeric Bases. Res J Pharm Technol 2020;13(12):6300–4.
[15] Jamal A, Alkawaz MH, Fatima M-A, Ab Yajid MS. In: 2019 IEEE 7th Conference on Systems, Process and Control (ICSPC). IEEE; 2019. p. 242–7.
[16] Xiang G, Gao X, Tang W, Jie X, Huang X. Numerical study on transition structures of oblique detonations with expansion wave from finite-length cowl. Phys Fluids 2020;32(5):056108.
[17] Miao R, Ma J, Liu Y, Liu Y, Yang Z, Guo M. Variability of aboveground litter inputs alters soil carbon and nitrogen in a coniferous–broadleaf mixed forest of Central China. Forests 2019;10(2).
[18] Ashouri M, Khoshkar Vandani AM, Mehrpooya M, Ahmadi MH, Abdollahpour A. Techno-economic assessment of a Kalina cycle driven by a parabolic Trough solar collector. Energy Convers Manage 2015;105:1328–39.
[19] Alhuyi Nazari M, Ahmadi MH, Ghasempour R, Shafii MB, Mahian O, Kalogirou S, et al. A review on pulsating heat pipes: from solar to cryogenic applications. Appl Energy 2018;222:475–84.
[20] Ahmadi MH, et al. Solar power technology for electricity generation: a critical review. Energy Sci Eng 2018;6(5):340–61. https://doi.org/10.1002/ese3.239.
[21] Elfaki AO, et al. Review and future directions of the automated validation in software product line engineering. J Theor Appl Inf Technol 2012;42(1):75–93.
[22] Aghayari R, Maddah H, Pourkiaei SM, Ahmadi MH, Chen L, Ghazvini M. Theoretical and experimental studies of heat transfer in a double-pipe heat exchanger equipped with twisted tape and nanofluid. Eur Phys J Plus 2020;135(2):252.
[23] Baghban A, Sasanipour J, Pourfayaz F, Ahmadi MH, Kasaeian A, Chamkha AJ, et al. Towards experimental and modeling study of heat transfer performance of water- SiO2 nanofluid in quadrangular cross-section channels. Eng Appl Computat Fluid Mech 2019;13(1):453–69.
[24] Wang N, Maleki A, Alhuyi Nazari M, Tlili I, Safdari Shadloo M. Thermal conductivity modeling of nanofluids contain MgO particles by employing different approaches. Symmetry 2020;12(2):206.
[25] Thalib MM, Vimala M, Manokar AM, Sathyamurthy R, Sadeghzadeh M, Sharifpur M. Energy, exergy and economic investigation of passive and active inclined solar still: experimental study. J Therm Anal Calorim 2021;145(3):1091–102.
[26] Eshgarf H, Kalbasi R, Maleki A, Shadloo MS, karimipour A. A review on the properties, preparation, models and stability of hybrid nanofluids to optimize energy consumption. J Therm Anal Calorim 2021;144(5):1959–83.
[27] Hajatzadeh Pordanjani A, Aghakhani S, Afrand M, Mahmoudi B, Mahian O, Wongwises S. An updated review on application of nanofluids in heat exchangers for saving energy. Energy Convers Manage 2019;198:111886.
[28] Ghalandari M, Maleki A, Haghighi A, Safdari Shadloo M, Alhuyi Nazari M, Tlili I. Applications of nanofluids containing carbon nanotubes in solar energy systems: a review. J Mol Liq 2020;313:113476.
[29] Watandost H, Achak J, Haqmal A. Oxidation of hydrogels based of sodium alginate and MnO2 as catalyst. Int J Innov Res Sci Stud 2021;4(4):191–9.
[30] Emrani A, Davoodnia A, Tavakoli-Hoseini Niloofar. Alumina supported ammonium dihydrogenphosphate (NH 4 H 2 PO 4/Al 2 O 3): Preparation, characterization and its application as catalyst in the synthesis of 1, 2, 4, 5-tetrasubstituted imidazoles,. Bull Korean Chem Soc 2011;32(7):2385–90.
[31] Tjahjono T, et al. Role of cryogenic cycling rejuvenation on flow behavior of ZrCuAlNiAg metallic glass at relaxation temperature. Trans Indian Inst Met 2021.
[32] Sanou Y, Samuel PT. The Comparative study of adsorption capacity of two mixed materials for arsenic remediation in aqueous solutions. J Environ Treat Tech 2021;9(3):559–65.
[33] Zhou B, et al. A Highly stretchable and sensitive strain sensor based on dopamine modified electrospun SEBS fibers and MWCNTs with carboxylation. Adv Electron Mater 2021;7(8):2100233. https://doi.org/10.1002/aelm.202100233.
[34] Hu L-B, et al. MoO3 Structures Transition from Nanoflowers to Nanorods and Their Sensing Performances; 2021.
[35] Mazraedoost S, Behbudi G. Basic nano magnetic particles and essential oils biological applications. J Environ Treat Tech 2021;9(3):609–20.
[36] Ferdous Azam SM, Yajid MSA, Khatibi A. Constructive dismissal doctrine: a case study of the selected malaysian industrial court cases from 1995 to 2004. Syst Rev Pharm 2020;11(1):827–33.
[37] Thomas P, Isa MZA. Factors Causing Ocular Injuries among Workers in Construction Industry in Malaysia.
[38] Khan J, Kusmahani SH, Ruhi S, Al-Dhalli S, Kaleemullah M, Saad R, et al. Design and evaluation of sustained release matrix tablet of flurbiprofen by using hydrophilic polymer and natural gum. Int J Med Toxocol Legal Med 2020;23(1 and 2):149. https://doi.org/10.5958/0974-4614.2020.00025.X.
[39] Ngafwan N, et al. Study on novel fluorescent carbon nanomaterials in food analysis; 2021.
[40] Hutapea S, et al. Study on food preservation materials based on nano-particle reagents; 2021.
[41] Bakhshkandi R, Ghoranneviss M. Investigating the synthesis and growth of titanium dioxide nanoparticles on a cobalt catalyst. J Res Sci, Eng Technol 2019;7(4):1–3.
[42] Saghiri S, Ebrahimi M, Bozorgmehr MRJCM. Electrochemical amplified sensor with mgo nanoparticle and ionic liquid a powerful strategy for methyldopa analysis. Chem Method 1999;5(3):234–9.
[43] Talavari A, Ghanavati B, Azimi A, Sayyahi S, B. Research. PVDF/MWCNT hollow fiber mixed matrix membranes for gas absorption by Al2O3 nanofluid. Progress Chem Biochem Res 2021:177–90.
[47] Bagheri S, Pormand E, Shariati S, Research B. Changes of the Saturated Hydraulic Conductivity of Soil Influenced and Exchangeable Sodium Percentage (% ESP),. 2 (42), p. 163-70.
[48] Esfe MH, Esfandeh S, Amiri MK, Afrand M. A novel applicable experimental study on the thermal behavior of SWCNTs(60%)-MgO(40%)/EG hybrid nanofluid by focusing on the thermal conductivity. Powder Technol 2019;342:998–1007.
[49] Hemmat Esfe M, Rahimi Raki H, Sarmasti Emami MR, Afrand M. Viscosity and rheological properties of antifreeze based nanofluid containing hybrid nano-powders of MWCNTs and TiO2 under different temperature conditions. Powder Technol 2019;342:808–16.
[50] Hemmat Esfe M, Rostamian H, Esfandeh S, Afrand M. Modeling and prediction of rheological behavior of Al2O3-MWCNT/5W50 hybrid nano-lubricant by artificial neural network using experimental data. Phys A 2018;510:625–34.
[51] Shahsavani E, Afrand M, Kalbasi R. Using experimental data to estimate the heat transfer and pressure drop of non-Newtonian nanofluid flow through a circular tube: Applicable for use in heat exchangers. Appl Therm Eng 2018;129:1573–81.
[52] Alnaqi AA, Aghakhani S, Pordanjani AH, Bakhtiari R, Asadi A, Tran M-D. Effects of magnetic field on the convective heat transfer rate and entropy generation of a nanofluid in an inclined square cavity equipped with a conductor fin: Considering the radiation effect. Int J Heat Mass Transfer 2019;133:256–67.
[53] Zheng Y, Yaghoubi S, Dezfulizadeh A, Aghakhani S, Karimipour A, Tlili I. Free convection/radiation and entropy generation analyses for nanofluid of inclined square enclosure with uniform magnetic field. J Therm Anal Calorim 2020;141(1):635–48.
[54] Bhattacharyya S, Pathak M, Sharifpur M, Chamoli S, Ewim DRE. Heat transfer and exergy analysis of solar air heater tube with helical corrugation and perforated circular disc inserts. J Therm Anal Calorim 2021;145(3):1019–34.
[55] Yan SR, Golzar A, Sharifpur M, Meyer JP, Liu DH, Afrand M. Effect of U-shaped absorber tube on thermal-hydraulic performance and efficiency of two-fluid parabolic solar collector containing two-phase hybrid non-Newtonian nanofluids. Int J Mech Sci 2020;185. Art. no. 105832.
[56] Komeilibirjandi A, Raffiee AH, Maleki A, Nazari MA, Shadloo MS. Thermal conductivity prediction of nanofluids containing CuO nanoparticles by using correlation and artificial neural network. J Therm Anal Calorim 2020;139(4):2679–89.

[57] Afrand M. Experimental study on thermal conductivity of ethylene glycol containing hybrid nano-additives and development of a new correlation. Appl Therm Eng 2017;110:1111–9.
[58] Ranjbarzadeh R, Akhgar A, Musivand S, Afrand M. Effects of graphene oxide-silicon oxide hybrid nanomaterials on rheological behavior of water at various time durations and temperatures: Synthesis, preparation and stability. Powder Technol 2018;335:375–87.
[59] Nazari MA, Ghasempour R, Ahmadi MH, Heydarian G, Shafii MB. Experimental investigation of graphene oxide nanofluid on heat transfer enhancement of pulsating heat pipe. Int Commun Heat Mass Transfer 2018;91:90–4.
[60] Skullong S, Promthaisong P, Promvonge P, Thianpong C, Pimsarn M. Thermal performance in solar air heater with perforated-winglet-type vortex generator. Sol Energy 2018;170:1101–17.
[61] Sheikholeslami M, Farshad SA. Investigation of solar collector system with turbulator considering hybrid nanoparticles. Renewable Energy 2021;171:1128–58.
[62] Sheikholeslami M, Farshad SA, Said Z. Analyzing entropy and thermal behavior of nanomaterial through solar collector involving new tapes. Int Commun Heat Mass Transfer 2021;123:105190.
[63] Saedodin S, Zaboli M, Ajarostaghi SSM. Hydrothermal analysis of heat transfer and thermal performance characteristics in a parabolic trough solar collector with Turbulence-Inducing elements. Sustainable Energy Technol Assess 2021;46:101266.
[64] Olfian H, Ajarostaghi SSM, Farhadi M, Ramiar A. Melting and solidification processes of phase change material in evacuated tube solar collector with U-shaped spirally corrugated tube. Appl Therm Eng 2021;182:116149.
[65] Farshad SA, Sheikholeslami M. Nanofluid flow inside a solar collector utilizing twisted tape considering exergy and entropy analysis. Renewable Energy 2019;141:246–58.
[66] Ebrahim Ghasemi S, Akbar Ranjbar A. Numerical thermal study on effect of porous rings on performance of solar parabolic trough collector. Appl Therm Eng 2017;118:807–16.
[67] Oztop HF, Bayrak F, Hepbasli A. Energetic and exergetic aspects of solar air heating (solar collector) systems. Renewable Sustainable Energy Rev 2013;21:59–83.
[68] Balaji K, Iniyan S, Muthusamyswami V. Experimental investigation on heat transfer and pumping power of forced circulation flat plate solar collector using heat transfer enhancer in absorber tube. Appl Therm Eng 2017;112:237–47.
[69] Acır A, Ata İ, Şahin İ. Energy and exergy analyses of a new solar air heater with circular-type turbulators having different relief angles. Int J Exergy 2016;20(1):85–104.
[70] Rostami S, Sepehrirad M, Dezfulizadeh A, Hussein AK, Shahsavar Goldanlou A, Shadloo MS. Exergy optimization of a solar collector in flat plate shape equipped with elliptical pipes filled with turbulent nanofluid flow: a study for thermal management. Water 2020;12(8):2294.
[71] Goldanlou AS, Sepehrirad M, Dezfulizadeh A, Golzar A, Badri M, Rostami S. Effects of using ferromagnetic hybrid nanofluid in an evacuated sweep-shape solar receiver. J Therm Anal Calorim 2021;143(2):1623–36.
[72] Nazir MS, Ghasemi A, Dezfulizadeh A, Abdalla AN. Numerical simulation of the performance of a novel parabolic solar receiver filled with nanofluid. J Therm Anal Calorim 2021;144(6):2653–64.
[73] Ma Y, Jamiatia M, Aghaei A, Sepehrirad M, Dezfulizadeh A, Afrand M. Effect of differentially heated tubes on natural convection heat transfer in a space between two adiabatic horizontal concentric cylinders using nano-fluid. Int J Mech Sci 2019;163:105148.
[74] Dezfulizadeh A, Aghaei A, Joshaghani AH, Najafizadeh MM. Exergy efficiency of a novel heat exchanger under MHD effects filled with water-based Cu–SiO 2-MWCNT ternary hybrid nanofluid based on empirical data. J Therm Anal Calorim 2021:1–24.
[75] Davarnejad R, Jamshidzadeh M. CFD modeling of heat transfer performance of MgO-water nanofluid under turbulent flow. Eng Sci Technol, Int J 2015;18(4):536–42.
[76] Behzadmehr A, Saffar-Avval M, Galanis N. Prediction of turbulent forced convection of a nanofluid in a tube with uniform heat flux using a two phase approach. Int J Heat Fluid Flow 2007;28(2):211–9.
[77] Hejazian M, Moraveji MK, Beheshti A. Comparative study of Euler and mixture models for turbulent flow of Al2O3 nanofluid inside a horizontal tube. Int Commun Heat Mass Transfer 2014;52:152–8.
[78] Göktepe S, Atalık K, Ertürk H. Comparison of single and two-phase models for nanofluid convection at the entrance of a uniformly heated tube. Int J Therm Sci 2014;80:83–92.
[79] Bahiraei M, Mazaheri N, Hosseini Y, Moayedi H. A two-phase simulation for analyzing thermohydraulic performance of Cu–water nanofluid within a square channel enhanced with 90° V-shaped ribs. Int J Heat Mass Transfwe 2019;145:118612.

Further reading

[44] Pordanjani AH, Aghakhani S. Numerical investigation of natural convection and irreversibilities between two inclined concentric cylinders in presence of uniform magnetic field and radiation. Heat Transfer Eng 2021:1–21.
[45] Tian M-W, Rostami S, Aghakhani S, Goldanlou AS, Qi C. A techno-economic investigation of 2D and 3D configurations of fins and their effects on heat sink efficiency of MHD hybrid nanofluid with slip and non-slip flow. Int J Mech Sci 2021;189:105975.
[46] Yan S-R, Aghakhani S, Karimipour A. Influence of a membrane on nanofluid heat transfer and irreversibilities inside a cavity with two constant-temperature semicircular sources on the lower wall: applicable to solar collectors. Phys Scr 2020;95(8):085702.